Mechanical behavior of fully-grouted bolt in jointed rocks subjected to double shear tests

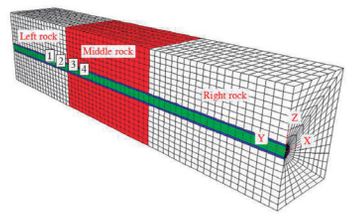

Comportamiento de un anclaje totalmente embutido en rocas adyacentes, sometido a ensayos de doble cortadura (cizallado)

Shuren Wang[1,2*], Huaiguang Xiao[2], Paul Hagan[3], and Zhengsheng Zou[1,2]

[1] International Joint Research Laboratory of Henan Province for Underground Space Development and Disaster Prevention, Henan Polytechnic University, Jiaozuo 454003, Henan, China
[2] Opening Laboratory for Deep Mine Construction, Henan Polytechnic University, Jiaozuo 454003, Henan, China
[3] School of Mining Engineering, The University of New South Wales, Sydney 2052, NSW, Australia
[*] Corresponding author, e-mail: w_sr88@163.com

DOI: http://dx.doi.org/10.6036/8325 | Recibido: 27/02/2017 • Evaluado: 27/01/2017 • Aceptado: 28/03/2017

RESUMEN

- Para analizar los resultados de un anclaje completamente embutido en rocas unidas se efectuaron ensayos de doble cizallado y se llevó a cabo la deducción analítica de la relación entre la fuerza axial, la fuerza de cizallado y el desplazamiento de cizallado del anclaje completamente embutido usando el modelo mecánico simplificado. Finalmente se analizaron las sensibilidades de los parámetros influyentes del anclaje. Los resultados muestran que la fuerza de cizallado predomina en el ensayo de cizallado que la fuerza de cizallado es mucho mayor que la fuerza axial. La fuerza de cizallado del anclaje completamente embutido aumenta cuando el incremento del desplazamiento del cizallado aumenta y la curva que relaciona la fuerza de cizallado y el desplazamiento de cizallado puede ser simplificada a cinco pasos: fuerte aumento, ligera disminución, suave aumento, suave disminución y muy fuerte disminución. Del mismo modo, las curvas de fuerza axial y de desplazamiento por cizallado pueden ser simplificadas a tres pasos: aumento estable, mantenimiento y fuerte disminución. Los resultados de la simulación muestran que el límite de tensión de la resistencia a cizalla del anclaje es el factor más significativo, la resistencia de las rocas unidas es el segundo y los parámetros de la superficie unida tienen el último efecto. Las conclusiones obtenidas en el estudio son de un valor teórico importante para la práctica de ingeniería similar.
- **Palabras clave:** Ensayo de doble cizallado, Anclaje completamente embutido, Fuerza axial, Fuerza de cizallado, Simulación numérica.

ABSTRACT

To analyze shear performances of the fully-grouted bolt in jointed rocks, the double shear tests were conducted, and the analytical derivation to the relationship among axial force, shear force and shear displacement of the fully-grouted bolt were carried out by using the simplified mechanical model. And the sensitivities of the influence parameters of the bolt were analyzed. The results show that the shear force predominates in the shear test and which is much greater than the axial force. The shear force of the fully-grouted bolt increases with the shear displacement increasing and the relationship curve of shear force and shear displacement can be simplified into five stages: steep increase, slight decline, slow increase, slow decline and sharp decline stages. Similarly, the axial force and shear displacement curve can be divided into three stages: stable increase, steady and sharp decline stages. The simulation results show that the confining pressure on the shear strength of the bolt is the most significant factor, the strength of the jointed rock is the second, and the jointed surface parameters show the least effect. The conclusions obtained in the study are of important theoretical value to direct the similar engineering practice.

Keywords: Double shear test, Fully-grouted bolt, Axial force, Shear force, Numerical simulation.

1. INTRODUCTION

For anchoring the fractured rock mass, the axial force and shear force of the bolt are not alone. The bolt not only can provide the strong tensile strength, but also can effectively prevent the separation of the rock mass when the jointed rock mass is strengthened by the fully-grouted bolt. The transverse shear behavior of the bolt often contributes greatly to the reinforcement effect of the rock mass. Many scholars focus too much on the axial force not considering the role of the shear force in valuating the bolt performance, so the current anchoring mechanism is far behind the engineering practice, which directly affects the rational application and development of the anchoring technology [1-3].

Since the existence of joints in the rock mass, the strength of the rock mass is often reduced and the jointed rocks are easy to move along the direction of the parallel or vertical to the joint face. The fully-grouted bolt in jointed rocks as an important support technology can effectively control the deformation and relative slippage of the jointed rocks. In many cases, the joint surface is not perpendicular to the axis direction of the bolt, so the bolt will be subjected to shear and tensile loading due to the rock moving along the plane of the jointed rocks [4-5]. Thus, it is necessary to evaluate the mechanical behavior of the fully-grouted bolt under shear and tensile loading conditions.

Due to the deformation of the rock mass is often controlled by the joints in the rock mass, the main motion of the rock is usual the shear displacement between the blocks, which leads to the supported bolts displaying the shear bend, cut, twist and pull off phenomenon. To analyze shear performances of the fully-grouted bolt in jointed rocks, this paper adopt the comprehension methods such as laboratory test, numerical simulation and theoretical analysis to research on the mechanical behaviors of the fully-grouted bolt in the jointed rocks subjected to double shear tests.

2. STATE OF THE ART

In recent years, research has confirmed that shear performance can be just as significant as tensile. So some scholars have conducted the analytical analysis of the shear force and the shear displacement, such as X.R. Ge and J.W. Liu analyzed the influence of rockbolt on the joint plane and reckoned formulas of the shear strength of the joint plane by laboratory tests and theoretical analysis [6]. K. Spang and P. Egger investigated the main parameters of rockbolt influence on joint plane and deduced formulas for the evaluation of the bearing capacity of the fully grouted bolts and for prediction of the required shear displacements [7]. Y.L. Wu et al. studied the interaction mechanism between the rockbolt and the jointed rock masses and analyzed the rockbolt influence on the stress intensity factor on the crack tip under tensile and shear forces by using linear elastic fracture mechanics [8]. S.L. Yang et al. proposed exponential function and parabolic function to describe the lateral shear stress of rockbolt and deduced the relationship between the shear force and the transverse displacement [9]. G. Grasselli simulated the shear tests of the jointed rock masses by a finite element model to reveal different deformations and shear forces of the full grouted bolt and the swelled bolt [10]. H. Jalaifar and N. Aziz pointed that bending behaviors of the bolt were divided into elastic and plastic phases under double shear tests with confining pressure, and he analyzed the influences on the joint plane position of plastic hinge, concrete strength, axial force and diameter of the bolt [11]. W. Zhang and Q.S. Liu established the deformation model under shear load and introduced length variable of extrusion failure to deduce the functional relations of shear-load versus shear displacement and axial-load versus axial displacement respectively [12]. F.L. Wang et al. studied the fully grouted bolt to support the bedding slope and established the linear functional relations between the shear effect of the bolt and the axial force of the bolt [13]. Other scholars have done many physical tests and numerical simulations in order to study the mechanical behavior of the rock bolt in resisting the shear force. Such as W. Wei et al. built the beam element model of the bolt near joint plane and developed the manifold simulated method base on the bolt model and the basic principle of numerical manifold [14]. Y. Chen conducted the optimized analysis of the influence factors on the jointed plane by laboratory tests for different setting angles, different block materials, and different joint displacements [15]. L. Li et al. simulated the relationships between shear force and shear displacement with different bolt setting angles, different rock strengths and different bolt diameters [16]. L.P. Srivastava and M. Singh stated that the rockbolt could increase strength of joint plane by large scale shear tests with non-confining and confining pressure [17], and the related research works [18-20], etc.

To sum up the above mentioned literatures, we found that many important results had been achieved about supporting parameters and mechanical behaviors of the rock bolt. However, it was not perfect enough about stress and deformation analysis of the bolt in the jointed rocks under double shear tests. So this paper would conduct further study to analyze the performances of the fully-grouted bolt in jointed rocks subjected to double shear tests. The remainder of this study was organized as follows. In Section 3, the comprehensive research methods, such as laboratory test, numerical simulation and theoretical analysis were introduced. In Section 4, the mechanical behaviors of the fully-grouted bolt under double shear tests were analyzed. Finally, some conclusions were given in Section 5.

3. METHODOLOGY

3.1. LABORATORY TEST

The double shear tests were conducted in the laboratory at School of Mining Engineering, The University of New South Wales, Australia.

3.1.1. Materials and specimens

As shown in Fig. 1(a), the basic materials included three concrete blocks to simulate the jointed rocks, cement covering the bolt to simulate the grout, and HRB steel bar to simulate the rock bolt. The steel plates located two lateral sides to distribute the axial loading stress evenly. The size of each block was 300 mm long, 300 mm wide and 200 mm high. The diameter of the steel bar was 16 mm, the diameter of the hole for the filled grout was 24 mm, and the thickness of the bottom steel plate was 20 mm.

3.1.2. Loading equipment and procedure requirements

As shown in Fig. 1(b), the capacity of the universal testing machine was 3600 kN, which was used to apply a vertical loading on the middle steel plate of the three ones located at the bottom of the test model from down to up. These FLA-3-11-3L resistance strain gauges were used to monitor the axial deformation of the grouted bolt and the strain gauge had a nominal resistance of 120 Ω and gauge factor of 2.12 ± 1%. The force senor located at the right side of the model and the liner displacement sensor (LVDT) in a fixed way were used to measure the axial force and shear displacement of the bolt, respectively.

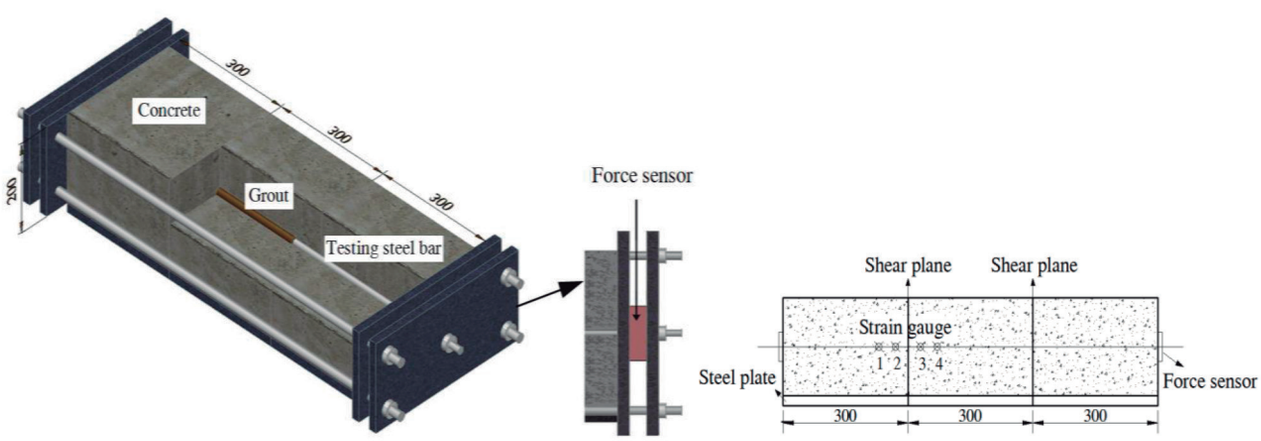

Fig. 1: The three-dimensional model and monitoring sensors of the model. (a) The three-dimensional model under double shear tests; (b) Loading direction and monitoring sensors of the model

As shown in Fig. 1(b), the strain gauges were set on the sides of the bolt (top and bottom), which were distanced from the jointed plane -70 mm, -30 mm, 30 mm, and 70 mm respectively. These positions of the strain gauges were marked by number 1 to 4. Due to the surface of the steel bar was not smooth enough, these positions of the strain gauges of the bolt were polished before setting strain gauges to ensure the measured data accurately. For maximizing the axial strain profiles, the strain gauges installed in the sample were aligned perpendicular to the shear load direction. This allowed analysis of the strains occurring on opposite sides of the rock bolt with expected zones of tension and compression.

In order to ensure all the three blocks bear stress evenly, three steel plates with 20 mm thickness were set up the downside of the three ones [16]. The left-end and right-end of the test model were fixed fully by the lock nuts, and the up and down directions of the middle block of the three ones were free. The universal machine could apply the vertical loading at the bottom of the middle block. When the applying load exceeded the maximum value of the capacity of the bolt, the test must stop.

The process of conducting such a test: Firstly, casting concrete blocks are needed before the test. Secondly, as shown in Fig. 1(a), three blocks are set on the bottom steel plate and the bolt with the strain gauges is set through these holes of three blocks. Thirdly, after the lateral steel plates and force sensors being set up, the left-end and right-end of the test model were fixed fully by the lock nuts. Fourthly, the model is moved to the universal testing machine and then can apply the vertical force up on the middle block to conduct the double shear test.

3.2. SIMPLIFIED MECHANICAL MODEL AND DERIVING FORMULAS

3.2.1. Engineering model

When the middle rock was applied the vertical up loading, the extruding force of the bolt appeared from the jointed plane. For the deformation development of the bolt firstly entered the small deformation and then failed to the large deformation phases, so the mechanical model would be divided into two phases: the elastic (small deformation) and the plastic (large deformation) phases.

To make the problem simpler, the simplified mechanical model was shown in Fig. 2(a), according to A.M. Ferrero's research results, the extruding force of the bolt presented the triangular distributing load [21]. But according to the views of Y.T. Liang, et al., when the deformation of the bolt was in the plastic stage, the extruding force of the bolt displayed a constant distributing load (Fig. 2(b)) [22].

3.2.2. Simplified mechanical model

Due to the extruding force of the bolt displayed the triangular distributing load in the elastic phase, the intersection point between the shear plane and the bolt was positioned *O* at the bolt. The deformation of the point *O* was zero, because the two sides of the shear plane were in pressure and tension zones respectively. According to stress analysis of the beam, the moment of point O was zero, so the point O just presented axial-force and shear-force. The moment of point C showed the maximum value and shear-force was zero, so the point C was the plastic hinge and point C could be simplified the fixed bearing, as shown in Fig. 3(a)(See section: supplementary material). Because the simplified model showed geometrical and mechanical symmetry, it could be simplified the statically determinate structure of a cantilever beam, as shown in Fig. 3(b) (See section: supplementary material).

As shown in Fig. 4(a) (See section: supplementary material), in the same way, when the mechanical model of the bolt was in the plastic phase, the simplified model could be simplified the statically determinate structure of a cantilever beam, as shown in Fig. 4(b) (See section: supplementary material).

3.2.3. Deriving the formulas for mechanical analysis

In the elastic phase, as shown in Fig. 3(b) (See section: supplementary material), according to the simplified mechanical model, we can write the following equations:

$$\begin{bmatrix} \delta_{11} & \delta_{12} & \delta_{13} \\ \delta_{21} & \delta_{22} & \delta_{23} \\ \delta_{31} & \delta_{32} & \delta_{33} \end{bmatrix} \begin{bmatrix} X_1 \\ X_2 \\ X_3 \end{bmatrix} + \begin{bmatrix} \Delta_{1q} \\ \Delta_{2q} \\ \Delta_{3q} \end{bmatrix} = \begin{bmatrix} \Delta_1 \\ \Delta_2 \\ \Delta_3 \end{bmatrix} \quad (1)$$

Where δ_{ij} was the displacement by unit force; X_1, X_2 and X_3 was axial-force, shear-force and moment of point 0, respectively. Δ_1, Δ_2, and Δ_3 was axial displacement, deflection, and rotation angle of point 0, respectively. Δ_{1q}, Δ_{2q} and Δ_{3q} was axial displacement, deflection and rotation angle of point 0 under the triangular distributed load, respectively.

According to the force method in structural mechanics, equations 2 and 3 can be obtained as follows:

$$\begin{bmatrix} \delta_{11} & \delta_{12} & \delta_{13} \\ \delta_{21} & \delta_{22} & \delta_{23} \\ \delta_{31} & \delta_{32} & \delta_{33} \end{bmatrix} = \begin{bmatrix} \frac{l_0}{EA} & 0 & 0 \\ 0 & \frac{l_0^3}{3EI} + \frac{kl_0}{GA} & \frac{l_0^2}{2EI} \\ 0 & \frac{l_0^2}{2EI} & \frac{l_0}{EI} \end{bmatrix} \quad (2)$$

$$\Delta_q = \begin{bmatrix} 0 \\ \frac{q_0 l_0^4}{12EI} + \frac{kql_0^2}{GA} \\ \frac{q_0 l_0^3}{9EI} \end{bmatrix} \quad (3)$$

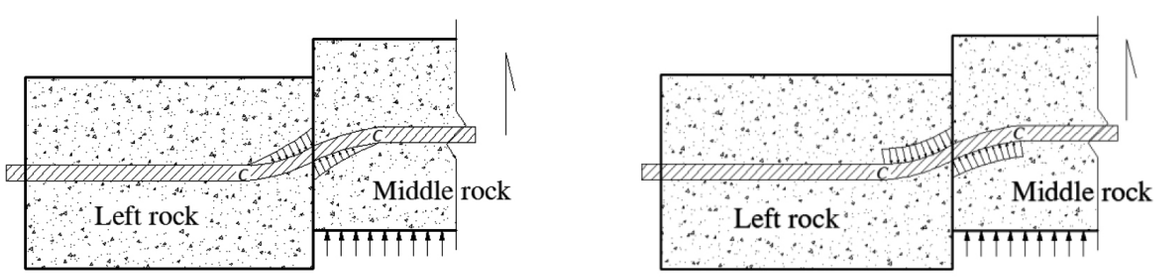

(a) *(b)*

Fig. 2: The different stress states of the bolt under double shear tests. (a) Elastic phase; (b) Plastic phase

Where l_0 was the stress length of the bolt. *E* was young modulus of the bolt. *G* was shear modulus of the bolt. *I* was the cross sectional moment of inertia of the bolt. *A* was the cross sectional area of the bolt. *k* was a concentration coefficient of the shear stress distribution.

Because the moment of point O is zero, and the deformation compatibility conditions were described as equation 4.

$$\begin{cases} \Delta_1 = u\sin\alpha \\ \Delta_2 = u \\ \Delta_3 = \alpha l \end{cases} \tag{4}$$

Where *u* was the loading displacement along the vertical direction and α was rotation angle of the bolt.

The axial-force of point O was written as equation 5.

$$X_1 = \frac{EA}{l_0}\Delta_1 \tag{5}$$

From equation 3, we can obtain the shear-force of point O and linear load as equations 6, 7, and 8.

$$X_2 = \frac{\left(18EIGAl_0^{\,2} + 72kE^2I^2\right)\Delta_3 - 24EIGAl_0\Delta_2}{12EIkl_0^{\,2} + GAl_0^{\,4}} \tag{6}$$

$$q_0 = \frac{-\left(216kE^2I^2 + 72EIGAl_0^{\,2}\right)\Delta_3 + 108EIGAl_0\Delta_2}{12kEIl_0^{\,3} + GAl_0^{\,5}} \tag{7}$$

$$X_2 = \frac{q_0 l_0}{2} \tag{8}$$

From equations 6 to 8, the relationship between Δ_2 and Δ_3 is written as equation 9.

$$\Delta_3 = \frac{13GAl_0}{30kEI + 9GAl_0^{\,2}}\Delta_2 \tag{9}$$

From equations 6 and 9, the shear-force of point O is written as equation 10.

$$X_2 = \frac{72kGAE^2I^2 + 6G^2A^2EIl_0^{\,2}}{\left(12EIkl_0 + GAl_0^{\,4}\right)\left(3GAl_0^{\,2} + 10kEI\right)}\Delta_2 \tag{10}$$

Then the axial-force of end of the bolt was

$$N_0 = X_1\cos\alpha \tag{11}$$

Similarly, in the plastic phase, as shown in Fig. 4(b) (See section: supplementary material), according to the simplified mechanical model, the analytical process was the same as that of the elastic phase.

The axial-force of point O is

$$X_1 = \frac{EA}{l_0}\Delta_1 \tag{12}$$

The axial-force of end of the bolt is the same as equation 11.

The shear-force of point O is

$$X_2 = \frac{576kGAE^2I^2 + 24G^2A^2EIl_0^{\,2}}{\left(24EIkl_0 + GAl_0^{\,4}\right)\left(11GAl_0^{\,2} + 40kEI\right)}\Delta_2 \tag{13}$$

3.3. BUILDING THE COMPUTATIONAL MODEL AND PROCEDURES

3.3.1 The computational model

According to the test model in the laboratory (Fig. 1), the computational model was built by using FLAC3D as shown in Fig. 5. Due to the geometrical symmetry of the test model, the computational model was simplified a half of the test model to improve the computational efficiency. There were three radcylinder models to simulate the three blocks in the test model, and the size of each radcylinder model was 300 mm long, 300 mm wide, and 200 mm high. The diameter of the bolt was 16 mm and a cshell model was 4 mm thickness to simulate the grout. There were three interfaces being embedded by rock to rock, rock to grout and grout to bolt to simulate the real interfaces.

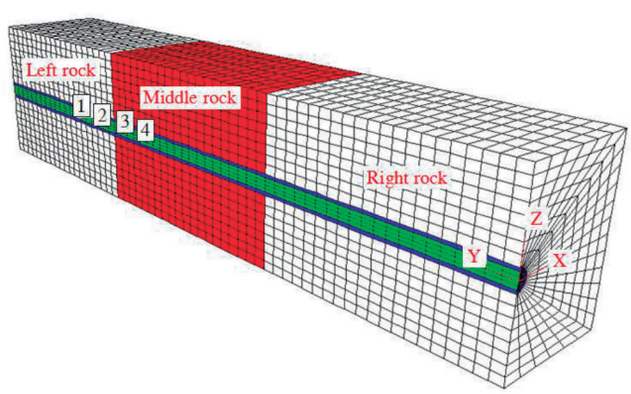

Fig. 5: The computational model and its meshes

3.3.2. Computational parameters and procedure requirements

The two lateral sides of the model were fixed fully in *y*- and *x*-axis directions respectively. The upper and the lower sides of the middle block were free while the other blocks were fixed at the two sides in *z*-axis direction.

Supposing the three blocks, the grout and the interfaces were followed Mohr-Coulomb's yield criterion. However, the bolt was regarded as a linear elastic body. The mechanical parameters of the model were listed in Tables 1 and 2.

Name	Bulk modulus (GPa)	Shear modulus (GPa)	Cohesion (MPa)	Friction angle (°)	Tension (MPa)
Rock	15.6	12.7	11	43	5
Grout	6.9	5.6	12	30	6
Bolt	77	43			

Table 1 The mechanical parameters of the model

During the computation, the middle rock was continuously applied the evenly distributed load. The bending displacements of the bolt were monitored at positions distanced from the joint plane were -70 mm, -30 mm, 30 mm, and 70 mm. The test did

Name	Normal stiffness (GPa/m)	Shear stiffness (GPa/m)	Cohesion (MPa)	Friction angle (°)
Rock-rock	2000	2000	0.1	20
Rock-grout	10000	10000	1.0	30
Grout-bolt	70000	70000	10	32

Table 2 The mechanical parameters of the interfaces

not stop until the bending displacements of the bolt without increasing.

4. RESULTS AND DISCUSSION

4.1. PERFERMANCES OF THE BOLT BASED ON THE TEST

As shown in Table 3, the tops of the bolt at position 1 and 2 being set ± 30 mm on distance from the shear plane displayed pressure stress. While the tops of the bolt at position 3 and 4 being set ± 70 mm on distance from the shear plane displayed tensile stress. In contrast, the stresses of the opposite side of these positions of the bolt showed the opposite stress state, but the deflection of the same position displayed nearly the same value.

Number of strain gauge	Deflection (mm)	Strain (10^{-3})	Distance from shear plane (mm)
1- Bottom	4.27	2.601 (+)	-70
1- Top	4.27	2.56 4 (-)	-70
2- Bottom	4.29	5.965 (+)	-30
2- Top	4.29	5.843 (-)	-30
3- Bottom	13.27	5.620 (-)	+30
3- Top	13.27	5.790 (+)	+30
4- Bottom	23.05	4.651 (-)	+70
4- Top	23.05	4.819 (+)	+70

Table 3 The measured strain and deflection of the bolt [16]

It can be seen from Fig. 6(a), at the elastic phase with initial loading, the shear-force increased dramatically while the shear displacement increased slowly. As the loading reached the elastic limit, the shear-force declined slightly before plastic stage. With the continuous loading, the deformation of the bolt was in the plastic stage, the shear-force increased slowly while the shear displacement increased largely. At last, the curve of shear-force and shear displacement displayed a dramatic decrease, as the rock was split suddenly with no stress force and this stage showed a sharp drop stage. In general, the shear-force of the fully-grouted bolt increased with the shear displacement increasing and the relationship curve of shear-force and shear displacement can be simplified into into five stages: steep increase, slight increase, slow increase, slow increase and sharp decline stages.

As seen from Fig. 6(b), when the middle block was applied the load by slowly lifting straight up, the bolt was restricted by both ends of the fixed steel plates and the axial-force of the bolt appeared. At first, with the shear displacement increasing, the axial force increased evenly. Then the axial force kept steadily with the shear displacement increasing. At last, the block was split, and the axial-force disappeared suddenly, so the curve of the axial force and shear displacement declined dramatically. Overall, the axial force of the fully-grouted bolt increased with the shear displacement increasing and this relationship curve of axial force and shear displacement can be simplified into three stages: stable increase, steady and sharp decline stages.

From the relationship curve of the shear force and the axial force (Fig. 7) (See section: supplementary material), without considering the initial loading fluctuation, we found that the shear force increased linearly with the axial force increasing. As shown in Fig. 8 (See section: supplementary material), it can be given a relationship curve between the bending displacement of the bolt and the positions distanced from the shear plane base the monitored data by LVDT. This curve described the upside of the bolt in left bock was in the compression zone and that in the middle block was in the tension zone.

4.2. ANALYTICAL SOLUTIONS FOR BEHAVIORS OF THE BOLT

According the test data (E=200 GPa, G=76.9 GPa, l_0=0.30 m, I =3.21×10^{-9} m^4, A =2×10^{-4} m^2, k =10/9), putting these parameters into formulas 10, 11, and 13, and then we can obtain the relationship of axial force, shear force and shear displacement in the elastic and plastic phases, respectively.

As shown in Fig. 9(a) (See section: supplementary material), it presented a similar trend between the analytical and test results. The axial force versus shear displacement curve displayed a straight line, because the variation of axial force is the same

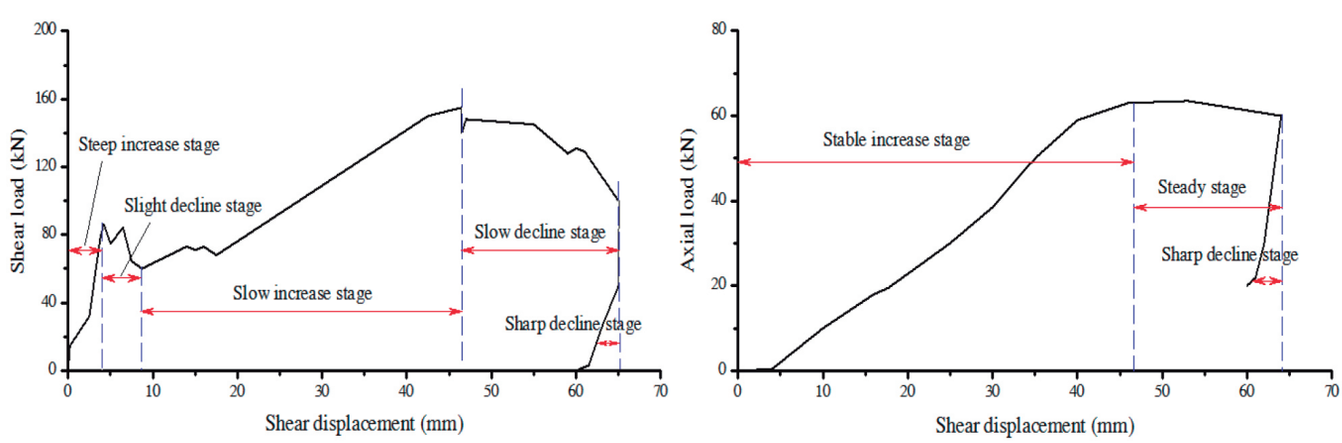

Fig. 6: The curves of shear force and axial force versus shear displacement under double shear tests. (a) The curve of shear force and shear displacement; (b) The curve of axial force and shear displacement

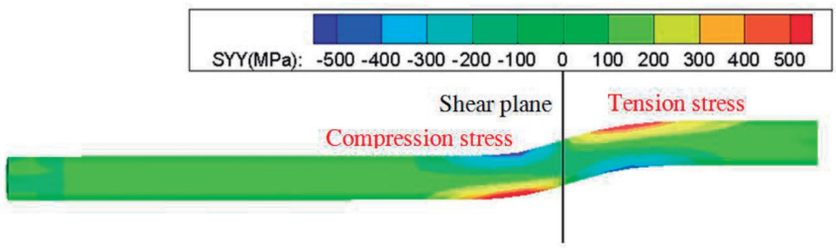

Fig. 11: The mechanical states of the bolt in the shear tests

in both the elastic and the plastic phases. In the cantilever beam model, it does not show the split phenomenon of the rock, so the analytical results do not appear the sharp decline trend. As shown in Fig. 9(b) (See section: supplementary material), the slope of the shear force is large in the elastic phase while that is small in the plastic phase in the analytical results, so the analytical curve presented the polyline segments. Similarly, the analytical results do not appear the sharp decline trend due to the non-split of rock in the analytical model.

4.3. NUMERICAL ANALYSIS OF PERFERMANCES OF THE BOLT

It can be seen from the displacement vectors field of the model (Fig. 10, see section: supplementary material), the middle rock displayed the vertical upward movement and the bolt showed both the vertical displacement and the axial displacement, which indicated that the bolt was subjected to shear stress and axial stress. As shown in Fig. 11, the upper part of the bolt on the left side nearby the shear plane displayed the compression stress, but that on the right side showed the tension stress. The lower parts of the bolt showed the opposite characteristics. The stress characteristics of the bolt were consistent with that in the physical test. As shown in Fig. 12 (See section: supplementary material), the bending displacement of the bolt in the numerical calculating was well consistent with that in the laboratory test in Table 3.

As shown in Fig. 13 (See section: supplementary material), the bending displacements of the bolt decreased with these parameters increasing, such as cohesion, friction and stiffness of rock-rock interface. As shown in Fig. 14 (See section: supplementary material), when S_{zz}=5.0 MPa and S_{xx}=5.0 MPa, the bending displacement of the bolt decreased significantly with the confining pressure of y-axis direction increasing. The results showed that the resistance ability of the shear plane increased with confining pressure increasing.

As the rock split under shear double tests due to scale effect, the bolt would not be in the pure shear stress state completely. However, this phenomenon can be reduced by increasing the scale of the test model. In this paper, only the stress state of the bolt under pure shear condition was taken into account. But in the practical engineering, the combination of shear and tension stress are combined. So in the next step, the combined stress states of the bolt along the joint surface will be further studied.

Because the loading process of the test was not completely in the static state, the force-displacement relationship displayed obviously curved characteristic, showing the dynamic loading characteristics. While the simplified analytical model was a static model, so the results showed a strong linear characteristics, but the relationship of force-displacement can have a good effect for the engineering design and construction.

Since the geological conditions are usually more complex, the fully-grouted bolt not only plays a role in resistance to tension, but also plays a role in shear. According to the rock strength, confining pressure and the parameters of the jointed plane, it is very important to choose optimized angles of the fully-grouted bolt to ensure the engineering safety.

5. CONCLUSIONS

To analyze the performances of the fully-grouted bolt in the jointed rocks subjected to the double shear tests, the comprehension methods such as laboratory test, numerical simulation and theoretical analysis were adopted. We obtained the conclusions as follows:

(1) Through the double shear tests of the bolt in the jointed rocks, we found that the shear force predominated in the shear test and the shear force was much greater than the axial force. The stress of the bolt on both sides of the jointed plane presented the opposite state, and the curve of shear force with shear displacement increasing displayed five stages: steep increase, slight decline, slow increase, slow decline and sharp decline stages. Similarly, the axial force and shear displacement curve can be simplified into three stages: stable increase, steady and sharp decline stages.

(2) Based on the results of laboratory tests, we found that the shear force increase linearly with the axial force increasing, and the elasto-plastic characteristics of the fully-grouted bolt under double shear tests were verified by the simplified analytical model. Moreover, the simulation results show that the confining pressure on the shear force of the bolt is the most significant factor, the strength of the jointed rock is the second, and the jointed surface parameters show the least effect.

It is not appropriate to focus too much on the axial force not considering the role of the shear force in valuating the bolt performance. The conclusions can greatly promote the sheared bolts application in anchoring the fractured rock mass. However, with the development of practice, the further studies are needed to consider the complicated conditions and more influencing factors to the shear force of the fully-grouted bolts.

BIBLIOGRAPHY

[1] Martin LB, Tijani M, Hadj-Hassen F. "A new analytical solution to the mechanical behaviour of fully grouted rockbolts subject to pull-out tests". Construction and Building Materials. February 2011. Vol. 25-2. P. 749-755. DOI: http://dx.doi.org/10.1016/j.conbuildmat.2010.07.011

[2] Wang SR, Xiao HG, Cao C, Zou ZS, Liu XL. "Simulation verification analysis of anchoring characteristics of transverse rib steel bar during pull-out test". DYNA. September 2016, Vol. 91-5. p. 548-553. DOI: http://dx.doi.org/10.6036/8077

[3] Chen JH, Saydam S, Hagan PC. "An analytical model of the load transfer behavior of fully grouted cable bolts". Construction and Building Materials. December 2015, Vol. 101-1. p. 1006-1015. DOI: http://dx.doi.org/10.1016/j.conbuildmat.2015.10.099

[4] Liu QS, Lei GF, Peng XX. "Advance and review on the anchoring mechanism in deep fractured rock mass". Chinese Journal of Rock Mechanics and Engineering. February 2016. Vol. 35-2. p. 312-332. DOI: http://dx.doi.org/10.13722/j.cnki.jrme.2015.0203

[5] Chen WQ, Jia ZX, Zhao YF, Liu LP, Zhou JJ, Lin XC. "Analysis of axial and transverse effects of rock bolt during shearing process". Rock and Soil Mechanics. January 2015. Vol. 36-1. p. 143-148. DOI: http://dx.doi.

org/10.16285/j.rsm.2015.01.020
[6] Ge XR, Liu JW. "Study on the shear resistance behavior of bolted rock joint". Chinese Journal of Geotechnical Engineering. February 1988. Vol. 10-1. p. 8-19.
[7] Spang K, Egger P. "Action of fully-grouted bolts in jointed rock and factors of influence". Rock Mechanics and Rock Engineering. July-September 1990. Vol. 23-3. p. 201-229.
[8] Wu YL, Wang YH, Xu MG. "Effect of bolt in jointed rock mass under mixed loading of tension and shearing". Chinese Rock Mechanics and Engineering. May 2003, Vol. 22-5. p. 769-772.
[9] Yang SL, Xu WY, Huang QP. "Analysis on the bolt deformation as result of joint shear displacement". Chinese Rock Mechanics and Engineering. October 2004. Vol. 23-19. p. 3268-3273.
[10] Grasselli G. "3D behaviour of bolted rock joints: experimental and numerical study". International Journal of Rock Mechanics & Mining Sciences. January 2005. Vol. 42-1. p. 13-24. DOI: http://dx.doi.org/10.1016/j.ijrmms.2004.06.003
[11] Jalalifar H, Aziz N. "Analytical behaviour of bolt-joint intersection under lateral loading conditions". Rock Mechanics and Rock Engineering. February 2010. Vol. 43-1. p. 89-94. DOI: http://dx.doi.org/10.1007/s00603-009-0032-6
[12] Zhang W, Liu QS. "Synthetical deformation analysis of anchor bolt in jointed rock mass". Rock and Soil Mechanics. April 2012. Vol. 33-4, p. 1067-1074.
[13] Wang FL, Liu CH, Gong Z. "Mechanisms of bolt support for bedding rock slopes".Chinese Journal of Rock Mechanics and Engineering. July 2014. Vol. 33-7. p. 1465-1470.
[14] Wei W, Jiang QH, Zhou CB. "A mechanical model of a bolt in the vicinity of a joint and its numerical manifold method (NMM) application". Engineering mechanics. November 2014. Vol. 31-11, p. 70-78. DOI: http://dx.doi.org/10.6052/j.issn.1000-4750.2013.01.0016
[15] Chen Y. "Experimental study and stress analysis of rock bolt anchorage performance". Journal of Rock Mechanics and Geotechnical Engineering. October 2014. Vol. 6-5, p. 428-437. DOI: http://dx.doi.org/10.1016/j.jrmge.2014.06.002
[16] Li L, Hagan PC, Saydam S, Hebblewhite B, Li Y. "Parametric study of rockbolt shear behaviour by double shear test". Rock Mechanics and Rock Engineering. July 2016. Vol. 49-12. p. 4787-4797. DOI: http://dx.doi.org/10.1007/s00603-016-1063-4
[17] Srivastava LP, Singh M. "Effect of fully grouted passive bolts on joint shear strength parameters in a blocky mass". Rock Mechanics and Rock Engineering. May 2015. Vol. 48-3. p. 1197-1206. DOI: http://dx.doi.org/10.1007/s00603-014-0615-8
[18] Li XW, Aziz N, Mirzaghorbanali A, Nemcik J. "Comparison of the shear test results of a cable bolt on three laboratory test apparatuses". Tunnelling and Undergroud Space Technology. January 2017. Vol. 61. p. 82-89. DOI: http://dx.doi.org/10.1016/j.tust.2016.10.003
[19] Gattesco N. Boem I. "Stress distribution among sheathing-to-frame nails of timber shear walls related to different base connections: Experimental tests and numerical modelling". Construction and Building Materials. September 2016. Vol. 122. p. 49-162. DOI: http://dx.doi.org/10.1016/j.conbuildmat.2016.06.079
[20] Wang SR, Hagan PC, Cao C. Advances in Rock-support and Geotechnical Engineering. Amsterdam: Butterworth-Heinemann, 2016. 410 p. ISBN: 978-0-12-810552-8
[21] Ferrero AM. "The shear strength of reinforced rock joints". International Journal of Rock Mechanics & Mining Science & Geomechanics Abstracts. September 1995. Vol. 32-6. p. 595-605. DOI: http://dx.doi.org/10.1016/0148-9062(95)00002-X
[22] Liang YT, He MC, Wang SR, Ren T. "A mechanical model for cone bolts". Computers and Geotechnics. March 2017. Vol. 83, p. 142-151. DOI: http://dx.doi.org/10.1016/j.compgeo.2016.10.017

ACKNOWLEDGEMENTS

This work was supported by the National Natural Science Foundation of China (51474188; 51474097; 51074140), the Natural Science Foundation of Hebei Province of China (E2014203012), the International Cooperation Project of Henan Science and Technology Department (162102410027), the Doctoral Fund of Henan Polytechnic University (B2015-67), and Program for Taihang Scholars.

SUPPLEMENTARY MATERIAL

http://www.revistadyna.com/documentos/pdfs/_adic/8325-1.pdf